Proceedings of ASME Turbo Expo 2011
GT2011
June 6-10, 2011, Vancouver, British Columbia, Canada

GT2011-45118

EFFECTS OF RIBS ON INTERNAL BLADE-TIP COOLING

Tareq Salameh and Bengt Sunden
Department of Energy Sciences, Division of Heat Transfer
Lund University, P.O. Box 118, SE-221 00 Lund, Sweden

ABSTRACT

This work concerns an experimental study of pressure drop and heat transfer for turbulent flow inside a U-duct with relevance for tip cooling of gas turbine blades. The U-duct models the internal blade cooling flow passages. Both friction factors and convective heat transfer coefficients were measured along the bend (turn) part of the U-duct for three different rib configuration cases, namely (a) single rib at three different rib positions, i.e., inlet, middle and outlet, (b) two ribs with three different configurations, i.e., at the inlet and middle, at the middle and outlet as well as at the inlet and outlet, and (c) three ribs. The rib height-to-hydraulic diameter ratio, e/D_h, was 0.1 and the pitch ratios were 10 and 20. The Reynolds number was varied from 8,000 to 20,000. The test rig has been built in such a way that various experimental setups can be handled as the bend (turn) part of the U-duct can easily be removed and the rib configurations can be changed. The surface temperature was measured by using a high-resolution measurement technique based on narrow band thermochromic liquid crystals (TLC R35C5W) and a CCD camera placed facing the bend (turn) part of the U-duct. The calibration of the TLC is based on the hue-based color decomposition system using an in-house designed calibration box. Both the friction factor and heat transfer coefficient were affected by the position and configuration of the ribs along the bend wall. The highest friction factor was found for two ribs placed at the middle and outlet positions of the bend wall, respectively. The highest heat transfer coefficient was found for two ribs placed at the inlet and middle positions of the bend wall, respectively. The uncertainties in the experiments were estimated to be 3% and 6% for the Nusselt number and friction factor, respectively.

1. INTRODUCTION

Roughness elements (ribs or turbulators) are used to enhance the heat transfer level in cooling passages where cooling is required. The ribs enhance the heat transfer process by restarting the boundary layer after flow reattachment between ribs. Many investigations have been performed to study both friction factor and heat transfer coefficients inside ribbed ducts. These studies are based on experimental or numerical techniques.

The experimental studies have been performed with various duct shapes. Some researchers used a straight duct to investigate the effect of several parameters on both the friction factor and heat transfer coefficient inside a gas turbine blade. Han et al. [1-4] studied the effect of aspect ratio, pitch ratio, rib height -to- hydraulic diameter ratio (blockage ratio), and rib angle of attack, respectively. Han and Zhang [5] and Taslim and Wadsworth [6] performed experimental studies to investigate the effect of the arrangement of the ribs inside the duct (aligned, V shape and staggered). In the study of Taslim et al. [7], the shape of the rib and bleed hole effects were obtained. The number of ribbed walls and the type of the ribs (continuous and truncated) effects were studied by Chandra et al. [8] and Wang and Sunden [9], respectively. In the study of Tanda and Cavallero [10], an optical technique to measure the heat transfer coefficient based on thermochromic liquid crystals (TLC) was used for the straight duct shape.

Other researchers used a fixed U bend (turn) duct, sometimes called a 180° sharp end duct, to study the effect of the bend (turn) part of U duct on local and spanwise heat transfer by using different experimental techniques. Johnson and Launder [11] measured the local heat transfer coefficients and temperature distributions for air flow around a 180° square-sectioned bend. In the study of Chyu [12], the heat transfer distributions were studied for flow passing through two-pass (one-turn) and three-pass (two-turn) passages by using the naphthalene mass transfer technique. Ekkad et al. [13] presented detailed heat transfer coefficient distributions for a two-pass square channel. One wall of the channel had periodically placed rib turbulators and bleed holes with four different configurations of the ribs (90° parallel, 60° parallel, 60° V and 60° inverted V) were considered. Mochizuki et al. [14] performed an experimental study to investigate heat transfer and fluid flow in two straight rectangular channels. Ribs were attached to two opposite walls with an angle of 90° or 60° to the flow. More than 450 thermocouples were used to monitor detailed distributions of local heat transfer coefficients over the four wall surfaces of the entire flow channel. The work by Astarita and Cardone [15] presented surface flow visualization, as well as local and spanwise averaged heat transfer measurements near a 180° sharp turn in a rectangular channel. Astarita et al. [16] measured detailed quantitative maps of the heat transfer distribution near a 180° sharp turn of a square

channel with rib turbulators by means of infrared thermography associated with the heated-thin-foil technique. Algawair et al. [17] performed an experimental study of the thermal development in a stationary cooling passage which consisted of two straight ducts of square cross section, with inclined ribs on two opposite sides connected by a square-ended U-bend. Salameh and Sunden [18] measured the friction factor and heat transfer coefficient inside a U-duct for three different cases, namely (a) the smooth straight part, (b) the smooth bend (turn) part, and (c) a rough (ribbed) bend (turn) part.

Most previous studies were related to the heat transfer on the leading and trailing walls of the two-pass channels, but very limited information is available for the tip wall. For these reasons, it is desirable to investigate more details of the heat transfer and pressure drop over tip walls. The objective of the present work is to study the heat transfer and pressure drop across the outer wall of the bend part (tip side of U-duct) for a smooth case and for different configurations with ribs.

2. EXPERIMENTAL APPARATUS AND PROCEDURES

2.1. Heat Transfer Test

2.1.1 Experimental Apparatus

Figure 1 shows the experimental apparatus used in this work. The apparatus consists of a U-duct with cross section area $50x50mm^2$. The U-duct walls are made in Acrylic material (thermal conductivity ($k= 0.2\ Wm^{-1}K^{-1}$)) to allow optical access for liquid crystal measurements. A suction fan was used to allow the air flow inside the U-duct. The illumination lighting, the charge coupled device (CCD) camera and the test section were covered by a dark enclosure to prevent background lighting influence.

The U-duct consists of a 1500 mm long straight part followed by a 240 mm inside length for the bend (turn) part. The ribs were placed transversely to the direction of the main flow at the outer wall of the bend (turn) part where the wall was heated by an electrical heater. The thickness of the U-duct wall is 20 mm while the hydraulic diameter D_h is 50 mm. The U-duct orientation is such that the rib-roughened wall is vertical allowing for positioning the CCD camera smoothly. Through the CCD camera, which allows 1024x512 pixels resolution with 256 grey levels per pixel, the temperature field is digitized and transferred through a frame grabber for storage and further image processing after steady state has been achieved. A narrow band liquid crystal sheet R35C5W (0.15 mm thick) backed with pressure-sensitive adhesive was employed to map the temperature distribution in the test region. Before performing the experiments, the liquid crystal was calibrated to get the calibration curve (montonic relationship) between the measured hue value and the value of the temperature. More details can be found in Gao [19]. An Inconel foil bonded on the top of a polyester film is applied to produce the uniform heat flux. The thickness of the Inconel foil is 12 μm, with relatively low thermal conductivity ($k=12\ Wm^{-1}K^{-1}$) and low temperature-dependent resistance of $1.25x10^{-4}1/°C$. The uniformity of the heat flux over the foil surface is typically within 1-2% of the average as in the study of Wiberg [20]. The heating foil was 50 mm wide and 240 mm long and covered the outer wall of the bend (turn) part (tip wall). The liquid crystal sheet was adhered on the outer surface of the heating foil. A schematic structure of THE liquid crystal and heater is shown in Fug. 2. The heat transfer measurements were performed at the test section of the duct where both flow and temperature fields are considered to be fully developed within the turbulent regime.

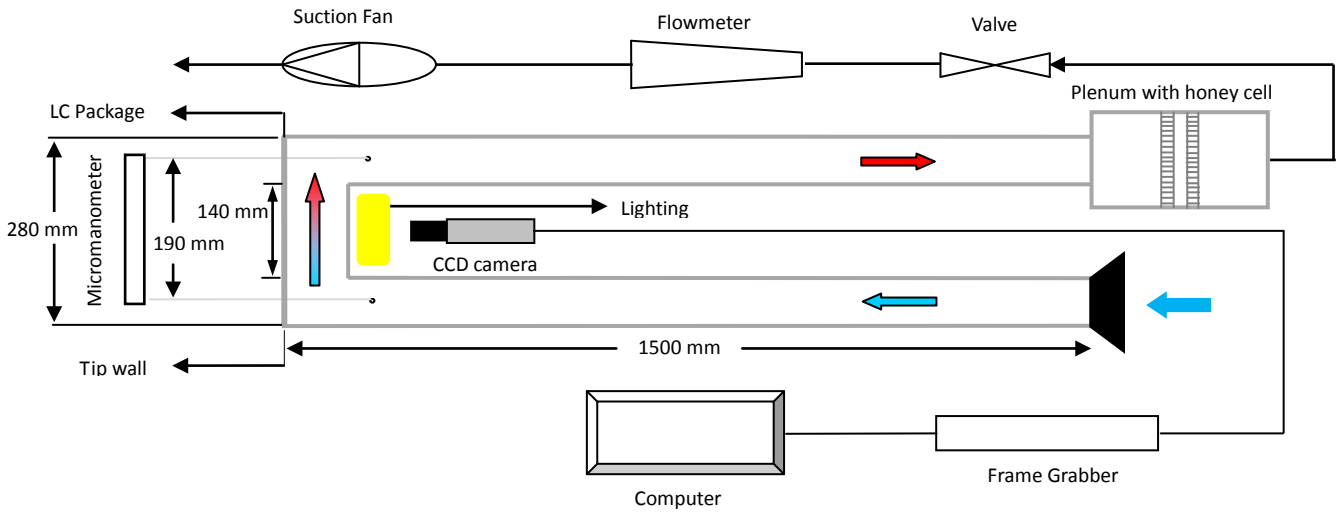

Figure 1. Schematics of experimental apparatus.

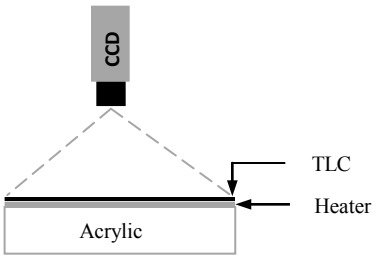

Figure 2. Schematics of liquid crystal and heater.

The ribs made of acrylic with square cross section (5 × 5 mm^2) are glued onto the outer wall of the bend (turn) part as shown in Fig. 3. The ribs were placed transversely to the direction of the main flow. The rib height-to-hydraulic diameter ratio, e/D_h, was 0.1 and the pitch ratios were 10 and 20.

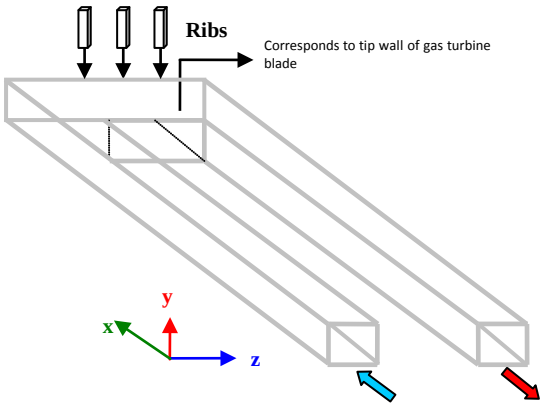

Figure 3. U-duct and positions of ribs.

The possible configurations of the ribs along the outer wall of the bend part of the U-duct are shown in Table 1.

Table 1. Configuration of the ribs along the outer wall of the bend (turn) part.

Rib #	Case #	Position at the outer wall of the bend (turn) part		
		Inlet	Middle	Outlet
1	i	x		
	ii		x	
	iii			x
2	i	x	x	
	ii		x	x
	iii	x		x
3	-	x	x	x

2.1.2 Experimental Procedure

During the experiments the air flow is measured with an error less than ±3%. Both current and voltage were used to calculate the electrical power supplied to the heater through a variable transformer so that the uniform heat flux to the wall could be varied as desired. The air temperature at the inlet of the U-duct was measured directly by a digital thermometer, with an accuracy of 0.03°C and a resolution of 0.01°C. The bulk air temperature inside the duct was evaluated by assuming a linear air temperature rise along the heated surface. At constant value of the air flow, the electrical power supplied to the heating foil was adjusted until the green colour appeared and covered the portion of the liquid crystal on the test section wall. When the green colour remained fixed without expansion, the images were taken by the CCD camera and were then transferred to the frame grabber for storage and further image processing. These images were converted from red, green and blue (RGB) matrices to hue, intensity and saturation (HIS) matrices. The hue value (H) was used to calculate the wall temperature by using the calibration curve. For each image the heat transfer coefficient can be calculated from the heat flux supplied, the surface temperature from the liquid crystal and the air bulk temperature.

2.2 Pressure Drop Test

The pressure drop test was performed in the same apparatus as for the heat transfer test except that there is no current passing through the heater. The static pressure taps were fixed across the total length of the bend (turn) part. The diameter of the tap holes is 1 mm. Short brass tubes were connected to the holes to provide connection with a micro manometer. The maximum error of the pressure drop was ±1%.

2.3 Data Reduction

The Reynolds number for the air flow inside a duct is defined in terms of mean velocity and hydraulic diameter as follows,

$$\mathrm{Re} = \frac{u_m D_h}{\nu} \qquad (1)$$

where ν is the air kinematic viscosity. The tests were performed for varying Re from 8,000 to 20,000.

The local Nusselt number, Nu, for heating air inside the duct can be derived directly from the heat flux and the temperature difference.

$$Nu = \frac{(Q_{el} - Q_{loss})D_h}{(T_w - T_{bulk})k_f A_s} \qquad (2)$$

where k_f is the air thermal conductivity and A is the area of the heating surface; T_w is the surface temperature indicated by the liquid crystal and T_{bulk} is the bulk temperature of the air at position x along the streamwise direction, Q_{el} is the measured electrical power supplied to the heater, Q_{loss} is the heat loss by radiative and conductive heat transfer. The sum of these two terms is found to be well below 3% of Q_{el} . The conduction heat loss was calculated from the temperature difference across the heated wall.

The air bulk temperature inside the duct can be calculated from an energy balance between the electrical power supply and the heat gain by the air as in equation (3).

$$T_{bulk} = T_{in} + (Q_{el} - Q_{loss})(X^{'}/L)/(\dot{m}c_p) \quad (3)$$

where T_{in} is the inlet air temperature measured at the entrance of the duct, c_p is the air specific heat, $\dot{m}$ is the mass flow rate, X' is a variable position along the heated surface, and L is the length of heated surface. Typically, the temperature difference between the wall and the bulk air is kept within 13-15°C. For all equations the air thermal properties were evaluated at the average air bulk temperature, see Holman [21].

The average Nusselt number can be calculated as in equation (4).

$$Nu_{av} = \frac{\sum_{i=1}^{N} Nu_i}{N} \quad (4)$$

where Nu_i is Nusselt number at local pixel and N is the number of pixels in the considered area.

It is important to note that in the present study, the ribs are made of acrylic and are not heated and thus not involved directly in the heat transfer process due to its low thermal conductivity and its small area compared with the total area of the heating surface. The ribs affect the forced flow and indirectly the heat transfer.

The friction factor f , based on isothermal conditions, can be represented by using the following definition as

$$f = (2\Delta P / L')(D_h / \rho u_m^2) \quad (5)$$

where ΔP is the pressure drop along the streamwise direction, $L^{'}$ is the distance between the two pressure taps, and ρ is the density of air.

All friction factors are normalized by the friction factor of a smooth circular tube, proposed by Blasius as (see Han [3]).

$$f_o = 0.046\,\mathrm{Re}^{-0.2} \quad (6)$$

The performance of the ribs is measured by using the performance index, PI, as (see Han [22]).

$$PI = \frac{Nu / Nu_o}{(f / f_o)^{1/3}} \quad (7)$$

2.4 Experimental uncertainty

During the experimental investigation, there are several parameters affecting the measured values such as electrical current passing through the heater, voltage across the heater, surface temperature measured by liquid crystal thermography, air bulk temperature, heat loss and flow meter readings. Based on the relative uncertainties of these parameters as shown in Table 2, an analysis of relative uncertainties was carried out for Reynolds number, friction factor and Nusselt number by using the following formulas.

$$\mathrm{Re} = \frac{\rho V D_h}{A_c\ \mu} \quad (8)$$

$$f = \frac{2\Delta p D_h^3}{L^{'}\ \rho V^2} \quad (9)$$

$$Nu = \frac{Q_{el}\ D_h}{A_s\ \Delta T\ k_a} \quad (10)$$

where V is the volumetric flow rate and ΔT is the temperature difference between the surface temperature measured by the liquid crystal thermography and air bulk temperature. The relative uncertainties were found to be ±3.5%, ±6% and ±3% for Reynolds number, friction factor and Nusselt number, respectively. The method in Moffat [23] was used in the analysis.

Table 2. Relative uncertainty for some measured parameters.

Measured parameter	Relative Uncertainty
Pressure Drop (Pa)	± 1%
Length (m)	± 0.5%
Volumetric flow rate (m^3/s)	± 3%
Temperature Difference (K)	± 0.3%
Electrical Power (W)	± 2%

3. RESULTS AND DISCUSSION

Both friction factors and convective heat transfer coefficients were measured inside the U-duct for different Reynolds numbers and rib configurations along the bend part, i.e., corresponding to the inside of the tip. Three different rib configuration cases, namely (a) single rib at three different rib positions, i.e., inlet, middle and outlet (b) two ribs with three different configurations, i.e., at the inlet and middle, at the middle and outlet as well as at the inlet and outlet, (c) three ribs, were tested along the outer wall of bend (turn) part. In the study of Salameh and Sunden [18], the friction factors and convective heat transfer coefficients were measured inside the smooth U-duct for different Reynolds numbers. All considered cases of rib configuration were compared with the smooth case.

Figure 3 shows a comparison between the area-average heat transfer coefficient enhancement factors for the smooth and different rib configurations along the bend part for varying Re number from 8000 to 20000. The fully developed duct Nu number was determined using the Dittus-Bolter correlation for symmetric heating, as shown in Holman [21], i.e., $Nu_o = 0.023\ Re^{0.8}\ Pr^{0.4}$. As seen from the figure, as the Re number increases, the heat transfer enhancement factor decreases. It is clear that the cases of two ribs at the inlet and the middle of the bend part and one rib at the outlet have the highest and lowest heat transfer enhancement factor respectively.

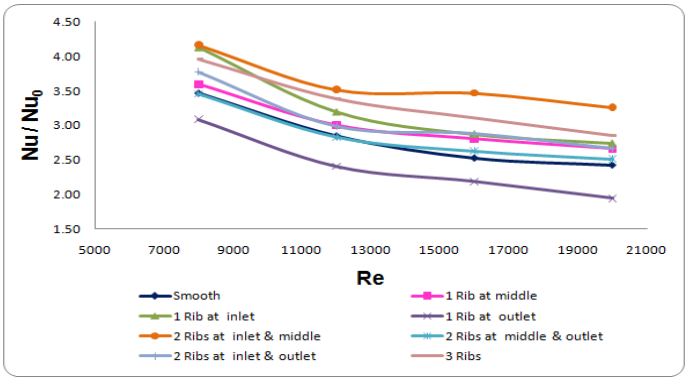

Figure 3. Area average Nusselt numbers for smooth and ribbed bend part cases.

Figure 4 shows normalized friction factors f / f_0 versus Re number for the smooth and different rib configurations along the bend part. For most cases, the pressure loss increases with increasing Re number, except for two cases, the two ribs at the inlet and middle positions of the bend wall, respectively, where the pressure loss decreases with increasing Re number, and the two ribs at the middle and outlet positions of the bend wall, respectively, where the pressure loss remains approximately constant. For most cases the pressure losses are higher than for the smooth case, except for the cases of one rib at the inlet and outlet at lower Reynolds numbers. The case of two ribs at the middle and outlet positions of the bend wall, respectively, has the highest pressure loss.

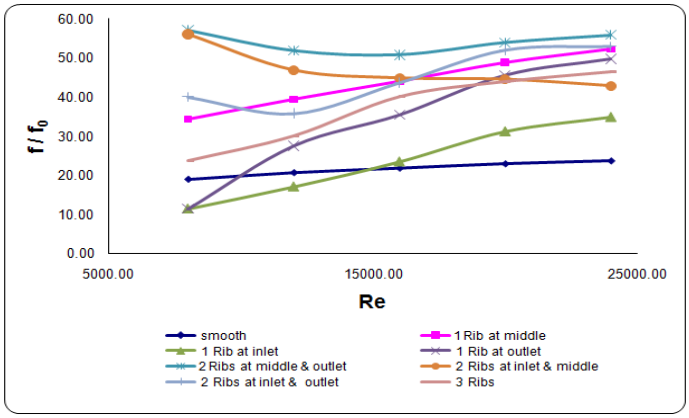

Figure 4. Normalized friction coefficient for smooth and ribbed bend parts cases.

Figure 5 shows the performance index PI versus Re number for all tested cases. The PI decreases with increasing Re number, the case of one rib at the inlet yield the highest performance index, while the cases of two ribs at the middle and outlet and one rib at the outlet have the lowest performance index, because these show up the largest pressure drop among all cases.

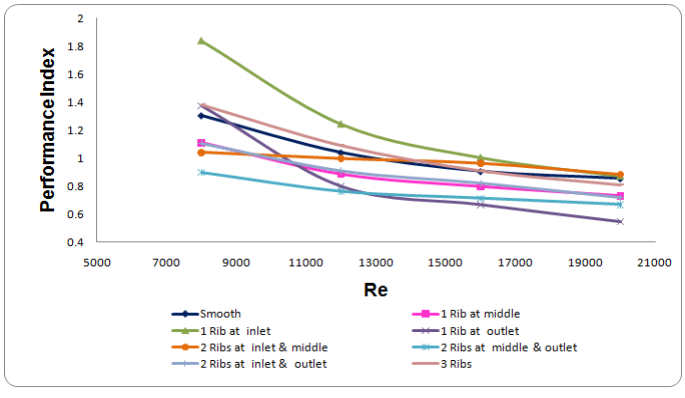

Figure 5. Performance index for smooth and ribbed bend parts cases.

Figures 6 and 7 provide two-dimensional Nu number distributions in the spanwise directions along the outer wall (tip wall) for all possible rib configurations. The distribution of Nu number is varying from one case to another. These variations depend on both the position and configuration along the bend (turn) part of the U-duct, and how the generated secondary flow affects the main flow stream to behaving for such a complex geometry as this cases. For the single rib case, the highest Nu number is found for the case of the rib placed at the inlet, while the lowest Nu number is found for the case of the rib placed at the outlet. For the two ribs case, the case with the two ribs placed at the inlet and middle positions of the bend wall gave the highest Nu number while the case of two ribs placed at the middle and the outlet positions of the bend wall gave the lowest Nu number. For the three ribs case, it is clear that, the case of three ribs is better than the case of two ribs at the inlet and outlet positions of the bend wall as shown by the distributions in the spanwise direction for both.

4. CONCLUSIONS

Narrow band liquid crystal thermography technique R35C5W LC was used to measured Nusselt number distributions inside a U-duct for different Reynolds numbers and rib configurations along the bend part, i.e., corresponding to the inside of the tip. A smooth tip, as well as tips with a single rib, two ribs and three ribs was considered. For the area average heat transfer coefficient enhancement factor, the case of two ribs at the inlet and middle positions of the bend wall, respectively, has the highest value, while the case of one rib at the outlet has the lowest value. For the pressure drop, the case of two ribs at the middle and outlet positions of the bend wall, respectively, has the largest pressure drop among all the cases, and the smooth case has the smallest pressure drop among them. The performance index for one rib at the inlet was the highest one, while the case of two ribs at the middle and outlet positions of the bend wall, respectively, presented the lowest value. It is worthwhile to mention that, the performance index for the case of two ribs at the inlet and middle of the bend wall, respectively, was approximately unity.

NOMENCLATURE

A_c = Cross section area of U- duct [m^2]
A_s = Surface heat transfer area [m^2]
c_p = Specific heat [J/kg.K]
D_h = Hydraulic diameter [m]
e = Rib height [m]
f = Fanning friction factor
f_0 = Fanning friction factor in smooth duct
h = Heat transfer coefficient [$W/m^2.K$]
k = Thermal conductivity [W/m .K]
k_f = Thermal conductivity of air [W/m.K]
L = Length of the heated surface [m]
L' = Distance between pressure taps [m]
$\dot{m}$ = Mass flow rate of air [kg/s]
N = Pixel number
Nu = Local Nusselt number
Nu_0 = Nusselt number in smooth straight duct
Nu_{av} =Average Nusselt number
ΔP = Pressure drop [Pa]
PI = Performance index
Pr = Prandtl number
Q_{el} = Electrical power supply [W]
Q_{loss} = Heat loss [W]
Re = Reynolds number
ΔT =Temperature difference [°C]
T_{bulk} = Air bulk temperature [°C]
T_{in} = Air inlet temperature [°C]
T_w = Wall temperature [°C]
u_m = Mean velocity [m/s]
V =Volumetric flow rate [m^3/s]
X = Streamwise direction [m]
X' = Variable position along the heater [m]
Y = Transverse direction [m]
Z = Spanwise direction [m]

Greek Symbols

ε = Emissivity
ν = Air kinematic viscosity [m^2/s]
ρ = Air density [kg/m^3]

ACKNOWLEDGMENTS

This work was carried out at the Division of Heat Transfer, Department of Energy Sciences, Faculty of Engineering, Lund University, Sweden. Financial support is provided by the Erasmus Mundus Windows Programme and the Swedish Energy Agency. Special thanks to our technician Mr. Ingjald Andréasson, who manufactured the experimental apparatus.

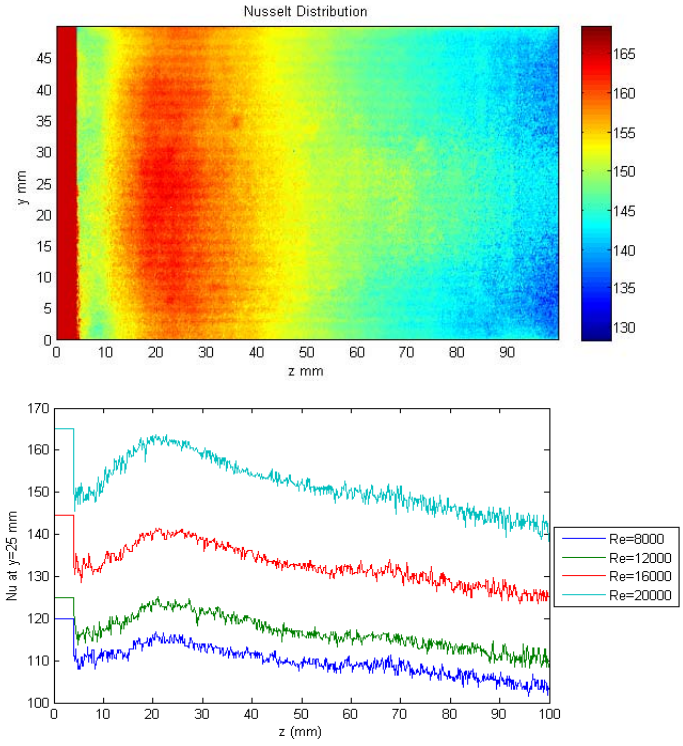

Single Rib case (i)

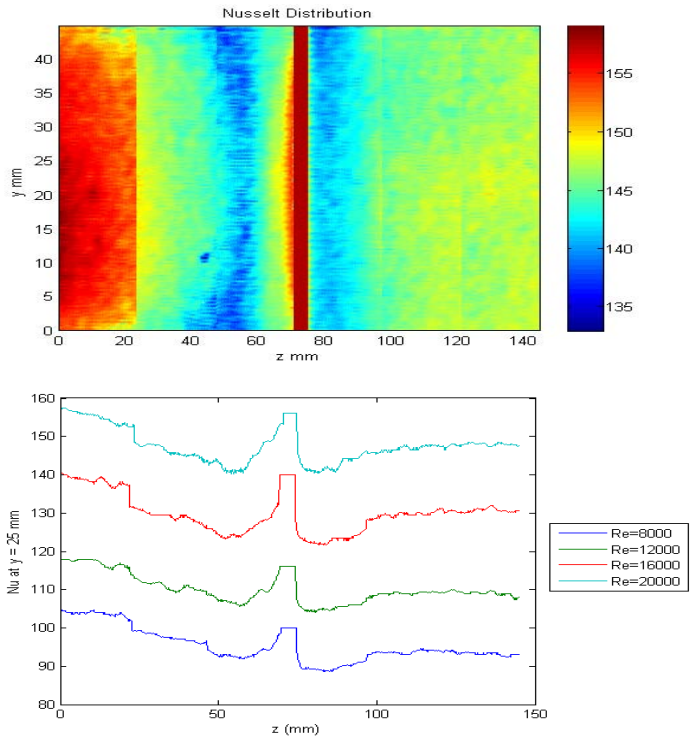

Single Rib case (ii)

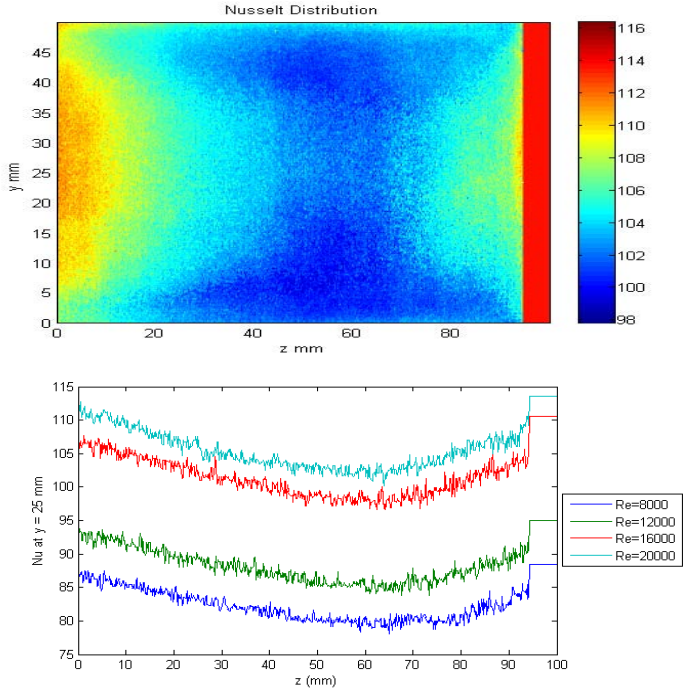

Single Rib case (iii)

Figure 6. Two dimensional Nusselt number distributions at Re=20000 in spanwise and flow directions for single rib.

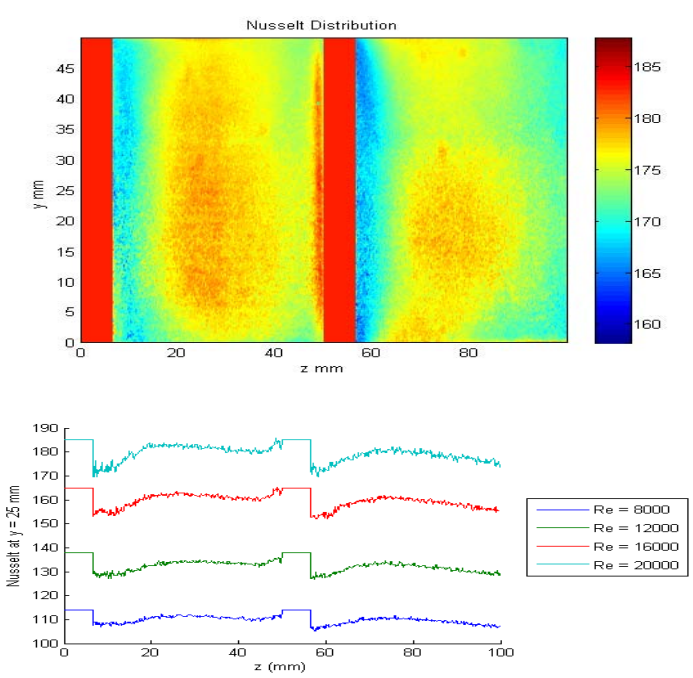

Two Ribs case (i)

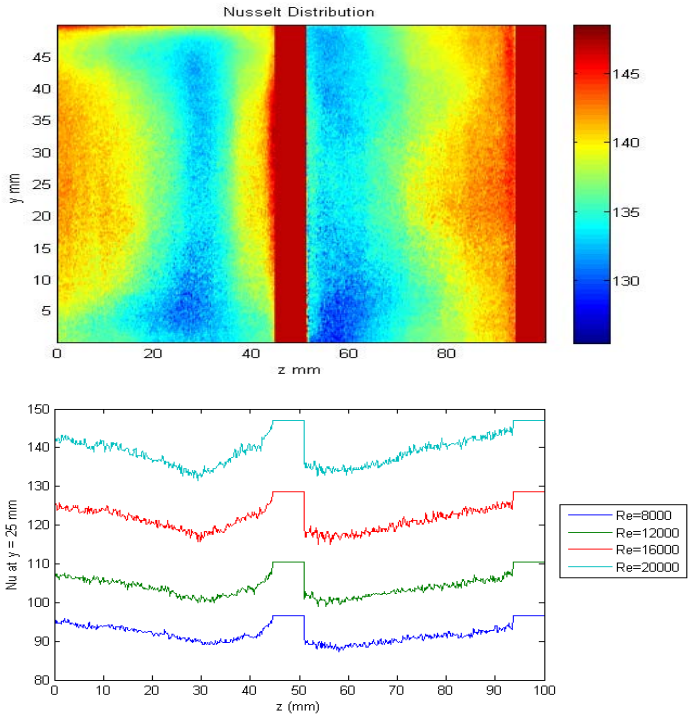

Two Ribs case (ii)

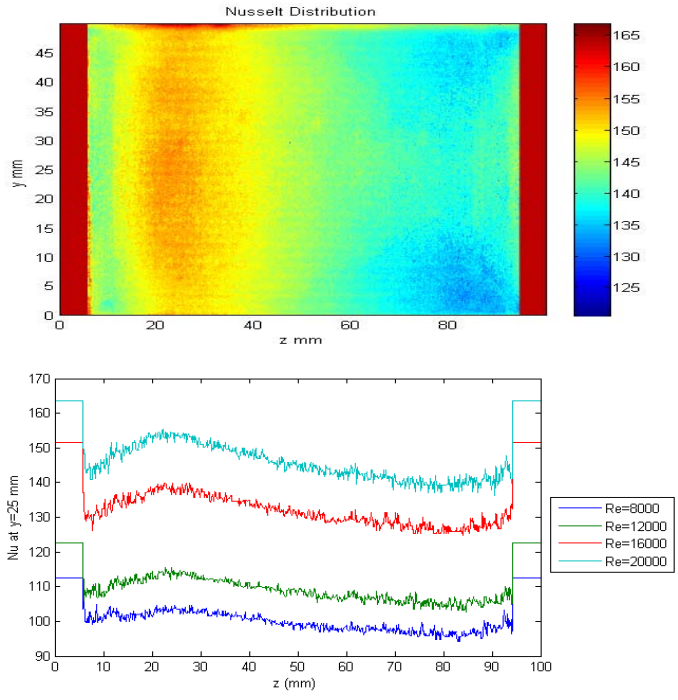

Two Ribs case (iii)

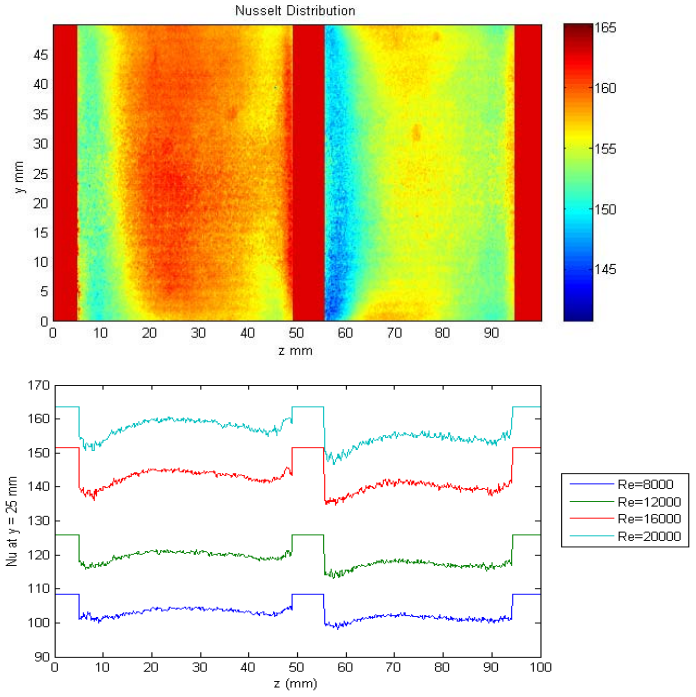

Three Ribs case

Figure 7. Two dimensional Nusselt number distributions at Re=20000 in spanwise and flow directions for two and three ribs.

REFERENCES

[1] Han, J. C., and Park, J. S., 1988, Developing Heat Transfer in Rectangular Channels with Rib Turbulators, International Journal Heat Mass Transfer, Vol. 31, No.1, pp. 183-195.

[2] Han, J. C., 1984, Heat Transfer and Friction on Channels With Two Opposite Rib-Roughened Walls, ASME Journal Heat Transfer, Vol. 106, pp. 774-781.

[3] Han, J.C., Ou S., Park, J.S., and Lei, C.K., 1989, Augmented heat transfer in rectangular channels of narrow aspect ratios with rib turbulators, International Journal Heat Mass Transfer, Vol. 32, pp. 1619-1630.

[4] Han J.C., Zhang Y.M., and Lee C.P., 1991, Augmented heat transfer in square channels with parallel, crossed, and V-shaped angled ribs, ASME Journal Heat Transfer Vol. 113, pp. 590-596.

[5] Han, J.C., and Zhang, Y.M., 1992, High performance heat transfer ducts with parallel, broken, and V-shaped ribs, International Journal Heat Mass Transfer, Vol. 35, pp. 513-523.

[6] Taslim, M.E., and Wadsworth, C.M, 1997, An experimental investigation of the rib surface-averaged heat transfer coefficient in a rib-roughened square passage, ASME Journal Turbomachinery, Vol. 119, pp. 381-389.

[7] Taslim, M.E., Li T., and Spring, S.D., 1995, Experimental study of the effects of bleed holes on heat transfer and pressure drop in trapezoidal passages with tapered turbulators, ASME Journal Turbomachinery, Vol. 117, pp. 281-290.

[8] Chandra, P.R., Niland, M.E., and Han J.C., 1997, Turbulent flow heat transfer and friction in a rectangular channel with varying number of ribbed walls, ASME Journal Turbomachinery, Vol. 119, pp. 374-380.

[9] Wang, L., and Sunden, B., 2005, Experimental investigation of local heat transfer in a square duct with continuous and truncated ribs, Journal Experimental Heat Transfer, Vol. 18, pp. 179-197.

[10] Tanda, G., and Cavallero, D., 2001, An experimental investigation of forced convection heat transfer in channel with rib turbulators by mean of liquid crystal thermography, Experimental Thermal Fluid Science, Vol. 26, pp. 15-121.

[11] Johnson, R. W., and Launder, B. E., 1985, Local Nusseit number and temperature field in turbulent flow through a heated square-sectioned U bend, International Journal Heat Fluid Flow, Vol. 6, pp. 171-180.

[12] Chyu, M.K., 1991, Regional heat transfer in two-pass and three-pass passages with 180° sharp turns, ASME Journal Heat Transfer, Vol. 113, pp. 63-70.

[13] Ekkad, S. V., Huang, Y., and Han, J.C., 1998, Detailed heat transfer distributions in two-pass square channels with rib turbulators and bleed holes, International Journal Heat Mass Transfer, Vol. 41, pp. 3781-3791.

[14] Mochizuki, S., Murata, A., Shibata, R., and Yang, W.J., 1999, Detailed measurements of local heat transfer coefficients in turbulent flow through smooth and rib-roughened serpentine passages with a 180° sharp bend, International Journal Heat Mass Transfer, Vol. 42 pp. 1925-1934.

[15] Astarita, T., and Cardone, G., 2000, Thermofluidynamic analysis of the flow near a sharp 180° turn channel, Experimental Thermal Fluid Science, Vol. 20, pp. 188-200.

[16] Astarita, T., Cardone, G., and Carlomagno, G. M., 2002, Convective heat transfer in ribbed channels with a 180° turn, Experiments in Fluids, Vol. 33, pp. 90-100.

[17] Algawair, W., Iacovides, H., Kounadis, D., and Xu, Z., 2007, Experimental assessment of the effects of Prandtl number and of a guide vane on the thermal development in a ribbed square-ended U-bend, Experimental Thermal Fluid Science, Vol. 32, pp. 670-681.

[18] Salameh, T., Sunden, B., 2010, An experimental study of heat transfer and pressure drop on the bend surface of a U-duct, ASME GT2010-22139, in Proceedings of ASME Turbo Expo 2010: Power for Land, Sea and Air GT2010, Glasgow, UK.

[19] Gao, X., 2002, Heat Transfer and Fluid Flow Investigation in Ribbed Duct and Impinging Jet Using Liquid Crystal Thermography and PIV, Ph.D. thesis, Division of Heat Transfer, Lund Institute of Technology , Lund, Sweden.

[20] Wiberg, R. 2004, A study of Heat Transfer From Cylinder in Turbulent Flow by Using Thermochromic Liquid Crystal, Licentiate thesis, Royal Institute of Technology, Stockholm, Sweden.

[21] Holman, J.P., Heat transfer, 9th ed., McGraw-Hill, New York, 2002.

[22] Han, J. C., Park, J. S., and Lei, C. K., 1985, Heat transfer enhancement in channels with turbulence promoters, ASME Journal Engineering for Gas Turbines and Power,107, pp. 628–635.

[23] Moffat, R. J., 1988, Describing the Uncertainty in Experimental Results, Experimental Thermal Fluid Science. Vol. 1, pp. 3-17.